UKRAINIAN CATHOLIC UNIVERSITY

BACHELOR THESIS

BLE phase shift and inertial sensor fusion for indoor localisation

Author:
Ostap DYHDALOVYCH

Supervisor:
Oleg FARENYUK

A thesis submitted in fulfillment of the requirements for the degree of Bachelor of Science

in the

Department of Computer Sciences
Faculty of Applied Sciences

Lviv 2022

Declaration of Authorship

I, Ostap DYHDALOVYCH, declare that this thesis titled, "BLE phase shift and inertial sensor fusion for indoor localisation" and the work presented in it are my own. I confirm that:

- This work was done wholly or mainly while in candidature for a research degree at this University.
- Where any part of this thesis has previously been submitted for a degree or any other qualification at this University or any other institution, this has been clearly stated.
- Where I have consulted the published work of others, this is always clearly attributed.
- Where I have quoted from the work of others, the source is always given. With the exception of such quotations, this thesis is entirely my own work.
- I have acknowledged all main sources of help.
- Where the thesis is based on work done by myself jointly with others, I have made clear exactly what was done by others and what I have contributed myself.

Signed:

Date:

"And it didn't stop being magic just because you found out how it was done"

Terry Pratchett

UKRAINIAN CATHOLIC UNIVERSITY

Faculty of Applied Sciences

Bachelor of Science

BLE phase shift and inertial sensor fusion for indoor localisation

by Ostap DYHDALOVYCH

Abstract

Indoor positioning has many real-life applications and currently is an actively researched topic. Due to the low cost and power consumption of Bluetooth Low Energy (BLE), as well as its prominent usage in common devices, it is an attractive technology to base localization on. A recent development in this field is a multi-carrier phase-based ranging solution. This thesis proposes a new positioning system that uses sensor fusion to combine phase-based BLE ranging data with inertial module measurements. The system is then tested in the simulated environment, showing high positioning accuracy.

Acknowledgements

I wish to express my gratitude to my supervisor, Oleg Farenyuk, for his constant guidance and support. I would also like to thank Oleh Kapshii and Ihor Kravets from Infineon Technologies Ukraine, who proposed the theme of this thesis and provided constructive feedback and valuable insights. Finally, I want to thank my physics teacher, Volodymyr Alekseychuk, for igniting my passion for understanding the world.

Contents

List of Figures

List of Abbreviations

BLE	**B**luetooth **L**ow **E**nergy
AP	**A**nchor **P**oint
IMU	**I**nertial **M**easurement **U**nit
RSS	**R**eceived **S**ignal **S**trength
ToA	**T**ime of **A**rrival
TDoA	**T**ime **D**ifference of **A**rrival
AoA	**A**ngle of **A**rrival
PDR	**P**edestrian **D**ead **R**eckoning

Chapter 1

Introduction

Determining a position of a certain device is required in many situations. If the device is outdoors, GPS is usually the best solution for this. However, inside buildings cannot provide reliable accuracy, so alternative solutions are required (Huang and Gartner, 2018). Bluetooth Low Energy (BLE) beacons are an attractive option for positioning due to their low power consumption, low cost, and ease of installation; however, the best BLE-based positioning approach is yet to be determined Jeon et al., 2018. Multi-carrier phase-based ranging is one of the most promising recent developments in this area, as it provides a reliable and noise-resistant way of measuring the distance to the beacons (Zand et al., 2019b). However, as of yet, no complete positioning system has been developed using this method.

1.1 Goals

Create a positioning system using phase-based BLE ranging that works well for indoor environments.

1.2 Thesis structure

Chapter 2. Related works

In this chapter, an overview of indoor positioning approaches is presented, with an emphasis on BLE-based positioning. Also, positioning approaches that incorporate inertial data are investigated.

Chapter 3. Background

Here, the background information related to the proposed system is provided.

Chapter 4. Proposed system

This chapter contains a detailed description of the proposed positioning system.

Chapter 5. Evaluation and results

This chapter describes an evaluation setup, and experimental results are presented.

Chapter 6. Summary

This chapter summarizes the work done and mentions possibilities for further development.

Chapter 2

Related Works

2.1 Indoor localisation techniques

As GPS positioning is generally unavailable indoors, many alternative technologies are being proposed for positioning. This includes visible light fingerprinting (Panta and Armstrong, 2012), magnetic field sensors (Ouyang and Abed-Meraim, 2022), ultrasound (Murata et al., 2014), and others. Radio wave-based systems such as Bluetooth, WiFi, and UWB are another prominently used group of technologies that, in general, provide the best compromise between costs, accuracy, coverage, and power consumption (Obeidat et al., 2021). As those technologies are all based on the same physical principles, they share the same main localization techniques listed below (Yassin et al., 2016).

1. Received Signal Strength (RSS): measurement of the relative strength of the signal sent from AP to the target device, which is correlated with distance. However, this requires a consistent signal fading model, so signal reflection and refraction can severely decrease localization accuracy.

2. RSS fingerprinting: Instead of using a theoretical model, signal strength data, known as RSS fingerprints, is collected from many locations inside the target environment beforehand. The RSS data received by the target device is then compared to those fingerprints to determine the location (Wen et al., 2015). This method achieves high positioning accuracy but requires time-consuming work of re-mapping all area when any anchor point is added or removed.

3. Time Of Arrival (ToA): measurement of the time needed for the signal to travel from the anchor points (AP) with a known location to the target device.

4. Time difference of arrival (TDoA): the difference in the signal travel time from each pair of APs is measured, thus eliminating the need for the synchronized time source.

5. Angle of Arrival (AoA): an angle at which the signal arrives to the target device is measured. This method potentially requires fewer devices, as only two APs are required for localization (Chen et al., 2012). However, a small error in angle determination can lead to a large error in the estimated position.

6. Phase-based ranging: the target method of this thesis; distance between APs and the target device is calculated based on the phase difference between the emitted and returned signal (Liu et al., 2014).

2.2 Phase-based BLE positioning

The phase-based ranging system was proposed in (Liu et al., 2014), with frequency-hopping to increase accuracy and mitigate radio interference. This idea is expanded on in (Zand et al., 2019b), with the ranging solution that is compatible with the BLE standards. (Zand et al., 2019a) optimizes positioning using this method by allowing the simultaneous distance estimation between several devices. In (Lu et al., 2021), phase-based BLE ranging is experimentally tested for indoor positioning, showing high localization accuracy.

2.3 Usage of filters for localisation

(Yim et al., 2008) is one of the first to use an extended Kalman filter for WLAN-based indoor positioning to increase positioning accuracy without fingerprinting. (Ye et al., 2019) uses a fusion algorithm based on the Kalman filter to combine AoA and RSS BLE methods with inertial sensor data to achieve positioning with only one anchor device. Many similar solutions utilize Pedestrian Dead Reckoning (PDR) (Kang and Han, 2014): human walking models that use IMUs to estimate the number and length of steps a person is taking to determine their movements. This data is then fused with other localisation technologies such as BLE for higher accuracy (Ciabattoni et al., 2019; Liao, Chiang, and Zhou, 2016; Zuo et al., 2018).

Chapter 3

Background

3.1 Phase-based localisation

3.1.1 Basic Idea

When traveling from one device to another, a phase shift of the radio signal is determined as follows:

$$\phi(x) = \frac{2\pi}{c} f x \pmod{2\pi}$$

where x is the traveled distance and f is the signal frequency. Thus, for a signal with the known frequency f_i, the traveled distance can be determined from its phase shift ϕ_i

$$x \left(\text{mod } \frac{c}{f_i}\right) = \frac{c\phi_i}{2\pi f_i}$$

The distance can only be determined up to the signal wavelength $\frac{c}{f_i}$ ($\approx 12.5cm$ for 2.4GHz BLE uses), so communication over multiple frequencies is needed for ranging over larger distances.

3.1.2 Combining multiple frequencies

Let us suppose that f is continuous over some interval $[f_0; f_0 + \Delta f]$; then, for a fixed distance x, the received signal value is:

$$I(f, x) = A \sin(\phi(f, x)) = A \sin\left(\frac{2\pi}{c} x * f\right).$$

In frequency domain its graph is a sine wave, with frequency $F_f(x) = \frac{x}{c}$ (Figure 3.1).

So, if phase shift data is available for a sufficient number of frequencies, a value of F_f can be obtained using the Fourier transform over the signal in frequency, and then the distance is calculated as $x = cF_f$ m.

3.1.3 Speed estimation

If a target is moving, received signal value changes over time as

$$I(f, t) = A \sin\left(\frac{2\pi f}{c} x(t)\right) = A \sin\left(\frac{2\pi f}{c} v_x * t\right)$$

where v_x is a target velocity x-axis projection relatively to the anchor point. Thus, target velocity can be estimated using Fourier transform over the signal in time.

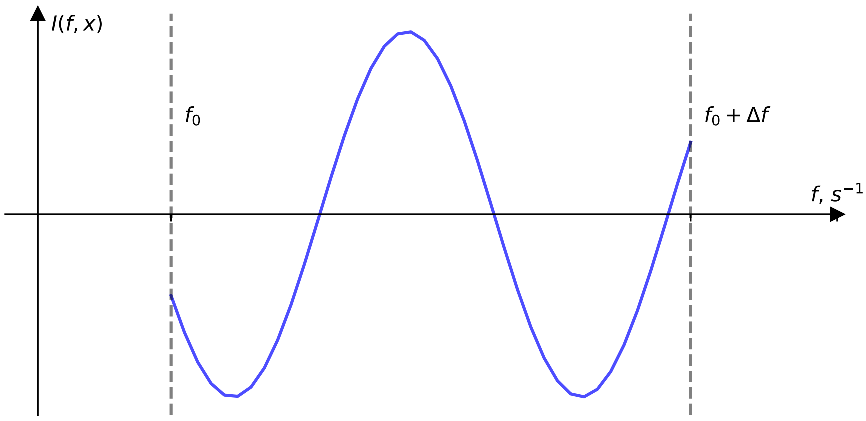

FIGURE 3.1: Signal in frequency domain with fixed x.

3.1.4 Multipath

In the indoor environment, a multipath effect is introduced: due to the reflection and refraction of the radio signals, the same packet from one device can reach the other via several paths of different lengths. In this case, the resulting signal is simply a sum of the signals from all paths.

$$I(f, \overline{x}) = \sum_i A_i \sin\left(\frac{2\pi}{c} x_i * f\right)$$

Fourier transform of this signal over f will result in a set of spikes, each corresponding to the length of one of the signal paths, with amplitudes proportional to the signal's amplitude. Usually, the direct path is the shortest and has the highest amplitude.

Similarly, Fourier transform of the signal over time will result in a set of velocities, each corresponding to length change speed of one of the signal paths.

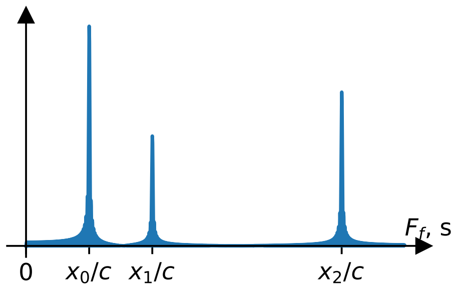

FIGURE 3.2: Fourier transform over f in case of multipath.

3.2 BLE

Bluetooth Low Energy (BLE) is a low-power wireless technology for short-range communication (Gomez, Oller, and Paradells, 2012). It was first introduced in 2009 in the Bluetooth Standard 4.0 (Woolley, 2019) as an energy-efficient alternative to the standard Bluetooth. While Bluetooth and BLE share many common characteristics, they are not mutually compatible.

3.2.1 Physical layer

BLE operates with a base frequency of 2.4 GHz, divided into 40 channels, each 2 MHz wide. Out of them, three (channels 37, 38, and 39 with frequencies 2402MHz, 2426MHz, and 2480MHz, respectively) are defined as advertising channels used for device discovery, connection, and broadcasting. Other 37 channels are used for communication to connected devices. To minimize signal interference, the frequency used for communication periodically changes, using an *adaptive frequency-hopping algorithm*.

Adaptive frequency hopping algorithm recursively calculates the next active channel index c_i as $c_i = (c_{i-1} + h) mod\ 37$, where c_{i-1} is the index of the previous active channel, and h is an integer between 5 and 16, that is constant for the duration of the BLE connection (Sarkar, Liu, and Jovanov, 2019). To prevent overlaps with other devices, another parameter m_c called channel map is used, which is set by the master device, and can be updated in the middle of connection using a (LL_CHANNEL_MAP_REQ) packet. It is a 40-bit value, that classifies each channel as ″used″ or ″unused″, depending on the wireless environment. If calculated channel c_i is ″unused″, the effective channel c'_i is computed as $(c_i) mod\ n_c$-th ″used″ channel, where n_c is a number of ″used″ channels in m_c. However, the calculation of the next channel c_{i+1} still depends on the c_i and not c'_i, so as to preserve the receptivity of channel selection.

3.2.2 Link layer

BLE communication can be carried out in two modes: advertisement and connection. In advertisement mode, one device (the advertiser) periodically broadcasts packets using one of the three advertising frequencies. It is most commonly used for device discovery, but it is also possible to perform positioning entirely in the advertising mode. Bluetooth 5 specification (Woolley, 2019) introduces a new advertising mode, that allows periodical advertisement packets AUX_SYNC_IND, hopping over 37 data channels. The scanner device can then reply to those packets with a SCAN_REQ command, thus enabling phase shift measurement and distance calculation (Zand et al., 2019b).

BLE device enters a connection mode when a listening device (called initiator) detects an active advertiser and sends a CONN_REQ command, establishing a two-way communication session with it. After the connection is established, communication between master and slave is divided into short time blocks called connection events. Each connection event is initiated by the master device and consists of one or several packet exchanges, during which both devices stay on the same frequency. At the start of a new connection event, both master and slave choose a new channel using a common pseudo-random algorithm. The time interval between two consecutive connection events (and thus between two frequency hops) is configured by the master device and can vary from 7.5ms to 4s. Thus, exchanging signals for all 37 data channels takes at least 277.5 ms for each device pair.

3.3 Sensor fusion

3.3.1 Overview

Sensor fusion is the process of combining information from multiple sensors, possibly of different nature, to obtain better results than each sensor could have provided independently (Gustafsson, 2010b). In the case of position estimation, this is usually achieved using the Bayesian approach – a probabilistic framework in which data from each sensor is used to update the estimated probability distribution of the tracked parameters, like target position or speed. Classical Bayesian fusion algorithms include:

- Kalman filter: the most basic algorithm that recursively updates probability distributions for linear Gaussian systems. For linear systems with additive Gaussian noise, it is proven to be the optimal estimator (Ribeiro, 2004).
- Extended Kalman filter: an application of the Kalman filter for non-linear models. It can produce good results for some non-linear systems but is not optimal in general.
- Unscented Kalman filter models the target probability distribution by updating a number of deterministically sampled points in the state space and approximating them by the Gaussian distribution (Wan and Van Der Merwe, 2000).
- Point-mass filter - grids the state space and discretizes the target probability distribution over this grid (Matoušek, Duník, and Straka, 2019). It can model any probability distribution but is limited by the memory consumption in the case of large-dimensional systems.

The features of the positioning system researched in this thesis, however, pose significant challenges in using this filters. The system is non-linear, as walking speed and direction may change constantly. The distance is measured to one anchor device at a time, resulting in non-Gaussian probability distributions; multipath effects and external interference may further complicate their shape. Luckily, there is another filter that provides accurate estimates for non-linear and non-Gaussian systems – the particle filter.

3.3.2 Particle filter

Particle filter (Gustafsson, 2010a) is a Monte-Carlo Bayesian fusion algorithm that models the target probability distribution using a large number of randomized particles. This allows the modeling of non-Gaussian distributions while also avoiding the high memory cost of grid-based approaches.

The algorithm starts by randomly generating a sample of particles. Each particle corresponds to a specific system state – for example, in the case of position determination, each particle will contain the target coordinates and moving direction. Each particle also has a weight variable that represents how well the particle fits the observed data. At the start, particle parameters are generated randomly, while weights are set to 1. Then, three steps are repeated for each piece of observed data (Fig.3.3).

1. **Predict**. Update coordinates of each particle according to the internal model. In the case of positioning, move each particle by estimated speed multiplied by elapsed time. To preserve sample variation, also change its orientation and position by some random values.
2. **Update**. Update the weight of each particle based on how well they fit the observed data, using a Bayes theorem. At the k-th step, the weight of i-th particle is calculated as

$$w_k^i = w_{k-1}^i P(z_k|\vec{x_k^i})$$

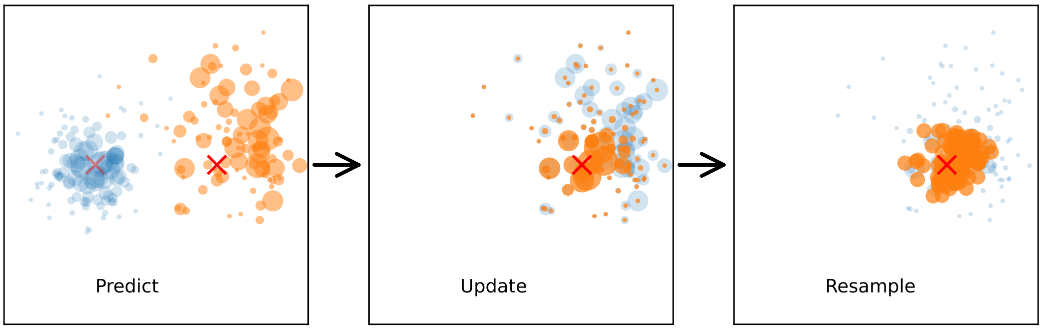

FIGURE 3.3: Particle filter stages illustration. Particles before each step are colored blue, particles after are orange. Particle weight is represented by the circle size.

where $P(z_k|\vec{x}_k^i)$ is a probability of obtaining measurement z_k given system state equal to $\vec{x}_k^i$, and w_{k-1}^i is particle weight at the previous iteration.

To prevent sample degeneracy (Li et al., 2014), **particle re-sampling** is preformed when particle weight distribution becomes too uniform. During it, some particles are dropped, and others are replicated at random, such that particles with bigger weight are more likely to be replicated, while particles with low weight are likely to be dropped. This results in a more compact sample, with more particles meaningfully contributing to position prediction.

3. **Estimate** Compute estimates for each parameter in the system by taking the weighted average of all particles.

$$\vec{\mu}_k = \frac{1}{N}\sum_{i=1}^{N} w_k^i \vec{x}_k^i$$

Chapter 4

Proposed system

4.1 Phase-based ranging

The basics of phase-based distance determination were laid out in the Background chapter. However, there still are some issues to be addressed.

Firstly, distance determination requires simultaneous data from all 37 channels, but due to the BLE constraints, phase shift data for each consecutive frequency is obtained with a 7.5ms delay after the previous one. Signal interpolation could mitigate this issue, but because of the small number of samples, it does not result in an accuracy improvement. On a small scale, phase shift linearly depends on the speed of a target device relative to the anchor (see 3.1.3), so system knowledge can be used to provide better interpolation; however, this is beyond the scope of this thesis.

Besides that, due to the adaptive frequency-hopping algorithm, some frequencies may be missing entirely. Luckily, the measurement density in the frequency domain is high enough for interpolation to be possible. At reasonable distances (0.5 - 10m), only two or less periods fit into the used frequency band (Fig. 4.1), so traditional signal interpolation techniques do not perform well. Instead, smooth cubic spline interpolation was used (Dierckx, 1995).

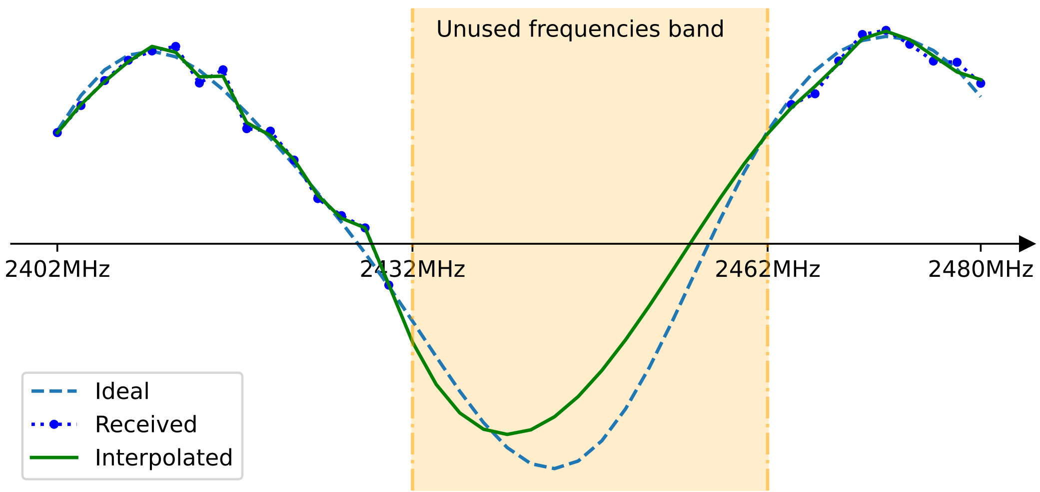

FIGURE 4.1: Frequency interpolation example at 5.1m distance. Frequencies from 2432MHz to 2462 MHz are considered "unused" because of the external interference.

Finally, a distance estimation must be computed from a continuous distribution obtained after the Fourier Transform. This can be done in several ways:

1. Largest peak: select the distance corresponding to the highest magnitude in the distribution. It is the easiest method that performs well enough in most situations. However, it has some important limitations. Firstly, in the presence of noise, the highest value can be shifted from the middle of the corresponding peak, resulting in lower difficulty. Moreover, suppose the direct signal path is suppressed (for example, by people standing in the way), and the reflected signals have high enough intensity. In that case, the distance estimation will be completely wrong.

2. First peak: identify some number of peaks, then select the one corresponding to the smallest distance. This method should yield better results in environments with a strong multipath effect as the direct path is the shortest. In the presence of noise, however, false peaks may be selected.

3. Weighted peaks: instead of only one distance, output several distances, with probabilities corresponding to their amplitudes. This method may better synergize with a particle used in the following steps, but the weight determination algorithm needs careful consideration: shorter distances must be preferred while also taking into account peak amplitudes and ignoring the baseline noise.

Out of those, the first peak method was used in the system. First, a moving average filter is applied to the data to reduce noise. Then, peaks are found as continuous sequences with magnitudes larger than the baseline. Finally, the largest value of the first detected peak is selected.

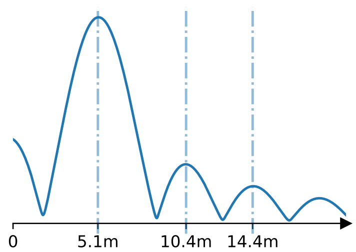

FIGURE 4.2: Three peaks selected, each corresponding to different paths.

4.2 IMU

IMU is primarily used for detecting direction changes and estimating walking speed.

Walking speed is estimated using Pedestrian Dead Reckoning, similarly to (Kang and Han, 2014). Moving average smoothing is used over acceleration data to reduce noise, and then peaks in acceleration are detected. Average speed is then computed as step length divided by the time between two consecutive peaks. For the sake of simplicity, step length is kept constant; if needed, it can be adjusted using the feedback from the particle filter.

Small direction changes can be inferred by the particle filter quite well, so only large changes have to be detected by the IMU. As high accuracy is not required, it is done using only gyroscope turning data.

4.3 Sensor fusion

To combine data from different sources, a particle filter was used. The high-level algorithm is as follows:

```
Create particles with random position and orientation;
while true do
    foreach anchor in anchorSet do
        Get signalData from anchor;
        // 278 ms
        Get speed and turn from IMU;
        if turn ≥ 45° then
            Change particles orientation by turn;
        end
        Change particles positions using speed;
        Estimate anchorDistance using signalData;
        Update particles weights according to anchorDistance;
        Resample particles;
        Estimate position as weighted average of particles;
    end
end
```

The estimated position is updated every time when phase shift data is obtained. Communicating on all 37 frequencies takes 277.5 ms, which means approximately three updates per second.

Chapter 5

Evaluation and results

5.1 Simulator

For testing the algorithm, a Python simulator was developed, covering both BLE and IMU data simulation. BLE simulation was based on the 1-dimensional MATLAB version provided by Infineon Technologies.

5.1.1 BLE simulation

BLE communication is modeled every 0.333 s, with one anchor device at a time. Communication is not instant: scanning each frequency takes 7.5 ms; frequency order is randomized. For each frequency, signal propagation through multiple paths is simulated and then added to obtain the final result. Signal amplitude is calculated using a free-space path-loss model: $A \sim \frac{1}{f_i x}$ (Debus and Axonn, 2006). Reflected signals additionally have their amplitude decreased by the factor of 0.4 (close to the empirical value for the concrete reflection coefficient at similar frequencies (Koppel et al., 2017)).

5.1.2 IMU simulation

IMU acceleration data is simulated based on the walking acceleration pattern shown in (Kang and Han, 2014). As only the distance between acceleration peaks is used by the positioning algorithm, the shape of peaks is kept simple: linear with randomized slopes and additive noise. When the target device changes direction, IMU rotations are reported to the system, with the added random noise around 30°.

5.2 Experiment and results

The target device is moving at a constant speed of 1 m/s and a constant height of 1 m in a rectangular room 5 by 6 meters. Both walls and floor reflect RF waves. Four anchor devices are positioned at the corners, at 2m height. Once every 3 s, a random interval of frequencies, with length of 5-10 channels, is selected to be "unused". In addition to signal reflections, a baseline noise is added to the signal data with a standard deviation of 0.002 (amplitude of an emitted signal at a 10m distance).

Two configurations of the system were tested: with and without IMU integration. Predicted positions can be seen on [5.1] and [5.3], with prediction errors on [5.4] and [5.2] (excluding first two predictions without enough information). At the start, when no knowledge of the system is available, the estimated position is close to (0,0); once data from enough anchors is received, the system reliably tracks the original path both with and without IMU, with a mean root square errors of 0.19m and 0.37m respectively. The main improvement IMU brings to the system is better direction change handling. However, experiments with real-world data are needed to verify this result.

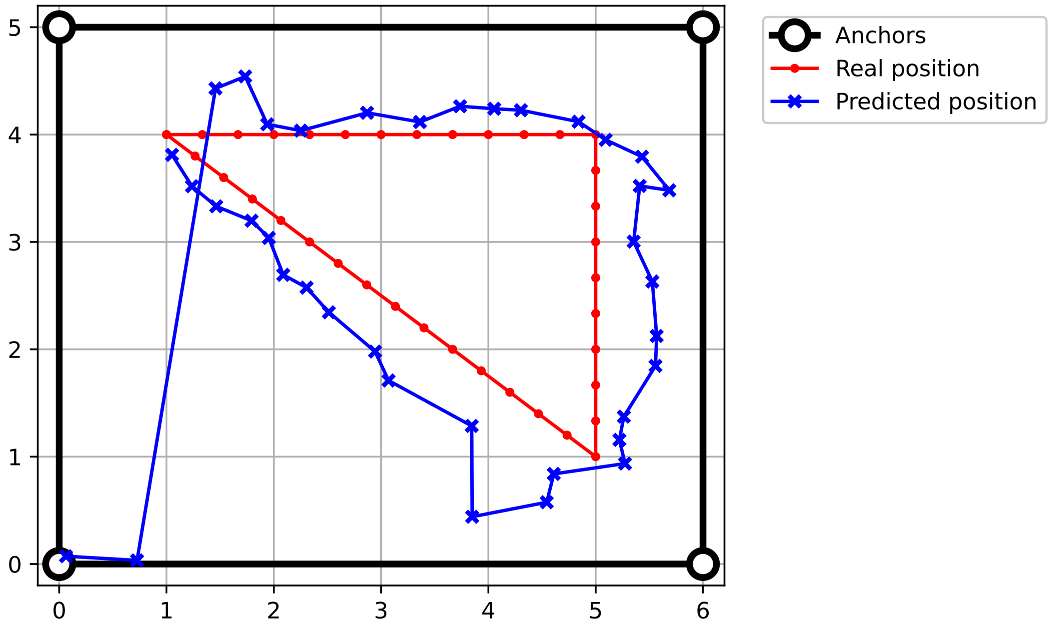

FIGURE 5.1: No IMU: predicted positions.

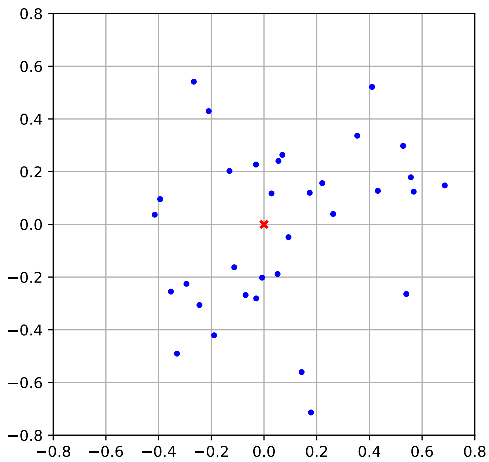

FIGURE 5.2: No IMU: positioning error.

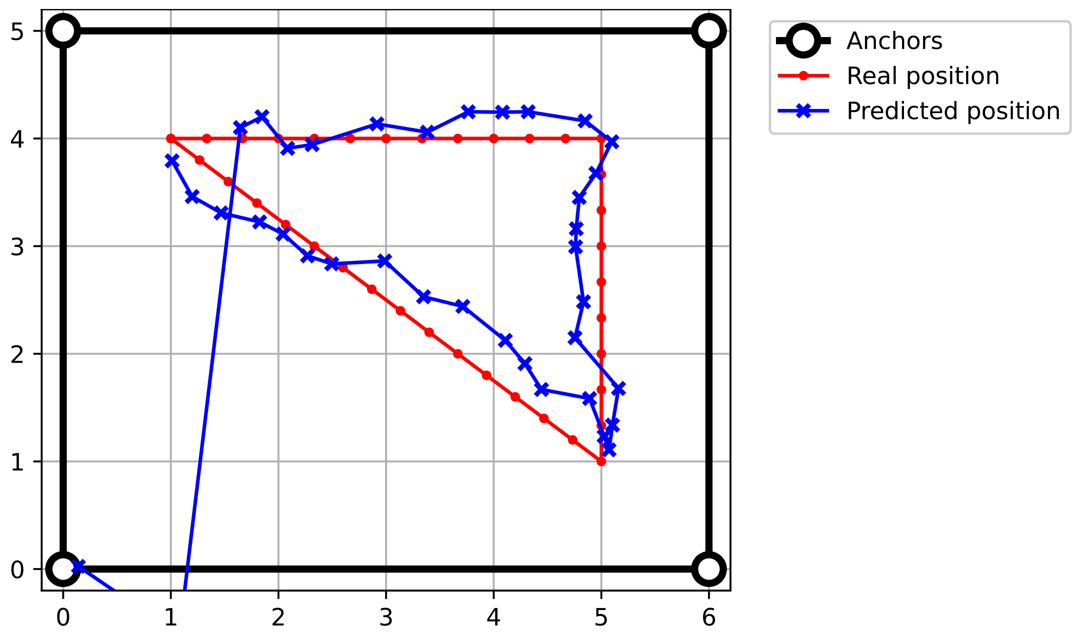

FIGURE 5.3: With IMU: predicted positions.

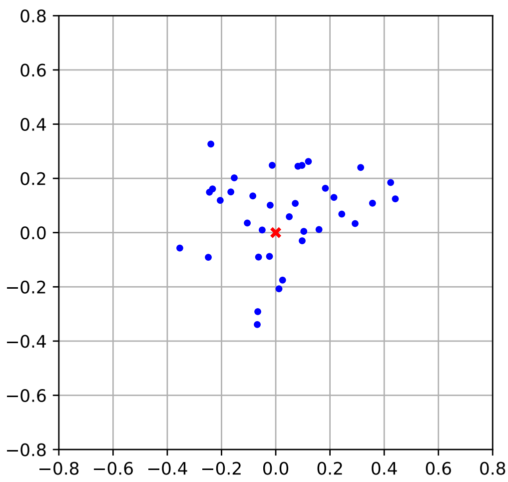

FIGURE 5.4: With IMU: positioning error.

Chapter 6

Summary

A new indoor positioning algorithm was developed by combining phase-based BLE ranging with IMU pedestrian tracking using a particle filter. The system shows high positioning accuracy in simulated experiments.

6.1 Future work

- Test the algorithm under real-world conditions.
- Improve IMU integration. Use a better algorithm for step detection and step length estimation; change estimated speed based on the particle filter feedback.
- Use a more advanced peak detection algorithm for BLE ranging. Possibly obtain several distances with different probabilities to use in the particle filter.

Bibliography

Chen, Hsieh-Chung et al. (2012). "Determining RF angle of arrival using COTS antenna arrays: A field evaluation". In: *MILCOM 2012 - 2012 IEEE Military Communications Conference*, pp. 1–6. DOI: 10.1109/MILCOM.2012.6415851.

Ciabattoni, Lucio et al. (2019). "Real time indoor localization integrating a model based pedestrian dead reckoning on smartphone and BLE beacons". In: *Journal of Ambient Intelligence and Humanized Computing* 10.1, pp. 1–12.

Debus, Walter and L Axonn (2006). "RF path loss & transmission distance calculations". In: *Axonn, LLC*.

Dierckx, Paul (1995). *Curve and surface fitting with splines*. Oxford University Press.

Gomez, Carles, Joaquim Oller, and Josep Paradells (2012). "Overview and evaluation of bluetooth low energy: An emerging low-power wireless technology". In: *Sensors* 12.9, pp. 11734–11753.

Gustafsson, Fredrik (2010a). "Particle filter theory and practice with positioning applications". In: *IEEE Aerospace and Electronic Systems Magazine* 25.7, pp. 53–82.

— (2010b). *Statistical sensor fusion*. Studentlitteratur.

Huang, Haosheng and Georg Gartner (2018). "Current trends and challenges in location-based services". In: *ISPRS International Journal of Geo-Information* 7.6, p. 199.

Jeon, Kang Eun et al. (2018). "Ble beacons for internet of things applications: Survey, challenges, and opportunities". In: *IEEE Internet of Things Journal* 5.2, pp. 811–828.

Kang, Wonho and Youngnam Han (2014). "SmartPDR: Smartphone-based pedestrian dead reckoning for indoor localization". In: *IEEE Sensors journal* 15.5, pp. 2906–2916.

Koppel, Tarmo et al. (2017). "Reflection and transmission properties of common construction materials at 2.4 GHz frequency". In: *Energy Procedia* 113, pp. 158–165.

Li, Tiancheng et al. (2014). "Fight sample degeneracy and impoverishment in particle filters: A review of intelligent approaches". In: *Expert Systems with applications* 41.8, pp. 3944–3954.

Liao, Jhen-Kai, Kai-Wei Chiang, and Zhi-Ming Zhou (2016). "The performance analysis of smartphone-based pedestrian dead reckoning and wireless locating technology for indoor navigation application". In: *Inventions* 1.4, p. 25.

Liu, Yue et al. (2014). "A phase-based ranging method for fast frequency hopping system". In: *2014 Sixth International Conference on Wireless Communications and Signal Processing (WCSP)*. IEEE, pp. 1–5.

Lu, Xingyu et al. (2021). "Indoor Positioning Experiment Based on Phase Ranging with Bluetooth Low Energy (BLE)". In: *Journal of Physics: Conference Series*. Vol. 1971. 1. IOP Publishing, p. 012044.

Matoušek, Jakub, J Duník, and Ondrej Straka (2019). "Point-mass filter: Density specific grid design and implementation". In: *Proceedings of the 15th European Workshop on Advanced Control and Diagnosis, Bologna, Italy*, pp. 21–22.

Murata, Shotaro et al. (2014). "Accurate indoor positioning system using near-ultrasonic sound from a smartphone". In: *2014 Eighth International Conference on Next Generation Mobile Apps, Services and Technologies*. IEEE, pp. 13–18.

Obeidat, Huthaifa et al. (2021). "A review of indoor localization techniques and wireless technologies". In: *Wireless Personal Communications* 119.1, pp. 289–327.

Ouyang, Guanglie and Karim Abed-Meraim (2022). "A Survey of Magnetic-Field-Based Indoor Localization". In: *Electronics* 11.6, p. 864.

Panta, Kusha and Jean Armstrong (2012). "Indoor localisation using white LEDs". In: *Electronics letters* 48.4, pp. 228–230.

Ribeiro, Maria Isabel (2004). "Kalman and extended kalman filters: Concept, derivation and properties". In: *Institute for Systems and Robotics* 43, p. 46.

Sarkar, Sopan, Jianqing Liu, and Emil Jovanov (2019). "A robust algorithm for sniffing ble long-lived connections in real-time". In: *2019 IEEE Global Communications Conference (GLOBECOM)*. IEEE, pp. 1–6.

Wan, Eric A and Rudolph Van Der Merwe (2000). "The unscented Kalman filter for nonlinear estimation". In: *Proceedings of the IEEE 2000 Adaptive Systems for Signal Processing, Communications, and Control Symposium (Cat. No. 00EX373)*. Ieee, pp. 153–158.

Wen, Yutian et al. (2015). "Fundamental limits of RSS fingerprinting based indoor localization". In: *2015 IEEE conference on computer communications (INFOCOM)*. IEEE, pp. 2479–2487.

Woolley, Martin (2019). "Bluetooth core specification v5. 1". In: *Bluetooth*.

Yassin, Ali et al. (2016). "Recent advances in indoor localization: A survey on theoretical approaches and applications". In: *IEEE Communications Surveys & Tutorials* 19.2, pp. 1327–1346.

Ye, Feng et al. (2019). "A low-cost single-anchor solution for indoor positioning using BLE and inertial sensor data". In: *IEEE Access* 7, pp. 162439–162453.

Yim, Jaegeol et al. (2008). "Extended Kalman filter for wireless LAN based indoor positioning". In: *Decision support systems* 45.4, pp. 960–971.

Zand, Pouria et al. (2019a). "A high-accuracy concurrent phase-based ranging for large-scale dense BLE network". In: *2019 IEEE 30th Annual International Symposium on Personal, Indoor and Mobile Radio Communications (PIMRC)*. IEEE, pp. 1–7.

Zand, Pouria et al. (2019b). "A high-accuracy phase-based ranging solution with Bluetooth Low Energy (BLE)". In: *2019 IEEE wireless communications and networking conference (WCNC)*. IEEE, pp. 1–8.

Zuo, Zheng et al. (2018). "Indoor positioning based on bluetooth low-energy beacons adopting graph optimization". In: *Sensors* 18.11, p. 3736.